Biochimica et Biophysica Acta 1827 (2013) 1235–1244

Contents lists available at ScienceDirect

Biochimica et Biophysica Acta

journal homepage: www.elsevier.com/locate/bbabio

Comparison of the physical characteristics of chlorosomes from three different phyla of green phototrophic bacteria

Peter G. Adams [a], Ashley J. Cadby [b], Benjamin Robinson [b], Yusuke Tsukatani [c], Marcus Tank [c], Jianzhong Wen [d,e], Robert E. Blankenship [d,e], Donald A. Bryant [c,f], C. Neil Hunter [a,*]

[a] Department of Molecular Biology and Biotechnology, University of Sheffield, Sheffield S10 2TN, UK
[b] Department of Physics and Astronomy, University of Sheffield, Sheffield S3 7RH, UK
[c] Department of Biochemistry and Molecular Biology, The Pennsylvania State University, University Park, PA 16802, USA
[d] Department of Biology, Washington University in St. Louis, St. Louis, MO 63130, USA
[e] Department of Chemistry, Washington University in St. Louis, St. Louis, MO 63130, USA
[f] Department of Chemistry and Biochemistry, Montana State University, Bozeman, MT 59717, USA

ARTICLE INFO

Article history:
Received 9 April 2013
Received in revised form 5 July 2013
Accepted 8 July 2013
Available online 16 July 2013

Keywords:
Bacterial photosynthesis
Light harvesting
Chlorosome
Atomic force microscopy
Fluorescence microscopy

ABSTRACT

Chlorosomes, the major antenna complexes in green sulphur bacteria, filamentous anoxygenic phototrophs, and phototrophic acidobacteria, are attached to the cytoplasmic side of the inner cell membrane and contain thousands of bacteriochlorophyll (BChl) molecules that harvest light and channel the energy to membrane-bound reaction centres. Chlorosomes from phototrophs representing three different phyla, *Chloroflexus* (*Cfx.*) *aurantiacus*, *Chlorobaculum* (*Cba.*) *tepidum* and the newly discovered "*Candidatus* (*Ca.*) Chloracidobacterium (Cab.) thermophilum" were analysed using PeakForce Tapping atomic force microscopy (PFT-AFM). Gentle PFT-AFM imaging in buffered solutions that maintained the chlorosomes in a near-native state revealed ellipsoids of variable size, with surface bumps and undulations that differ between individual chlorosomes. *Cba. tepidum* chlorosomes were the largest (133 × 57 × 36 nm; 141,000 nm^3 volume), compared with chlorosomes from *Cfx. aurantiacus* (120 × 44 × 30 nm; 84,000 nm^3) and *Ca.* Cab. thermophilum (99 × 40 × 31 nm; 65,000 nm^3). Reflecting the contributions of thousands of pigment–pigment stacking interactions to the stability of these supramolecular assemblies, analysis by nanomechanical mapping shows that chlorosomes are highly stable and that their integrity is disrupted only by very strong forces of 1000–2000 pN. AFM topographs of *Ca.* Cab. thermophilum chlorosomes that had retained their attachment to the cytoplasmic membrane showed that this membrane dynamically changes shape and is composed of protrusions of up to 30 nm wide and 6 nm above the mica support, possibly representing different protein domains. Spectral imaging revealed significant heterogeneity in the fluorescence emission of individual chlorosomes, likely reflecting the variations in BChl *c* homolog composition and internal arrangements of the stacked BChls within each chlorosome.

1. Introduction

Chlorosomes, the largest photosynthetic light-harvesting antenna complexes known, are elongated structures consisting of aggregates of up to 250,000 BChl pigments attached to the cytoplasmic side of the inner cell membrane. The dense packing of BChl molecules results in highly efficient capture of light energy and its channelling towards membrane-embedded light-harvesting/reaction centre (LH/RC) pigment–protein complexes. This fundamentally different LH antenna, in which there is minimal involvement of proteins, in contrast to the strict membrane protein–pigment relationship found in other photosynthetic systems, allows chlorosome-containing phototrophs to survive in some of the most extreme, light-poor environments in the world. Several reviews on chlorosomes are available [1–4].

Chlorosomes were first discovered in green sulphur bacteria (GSB), in *Chlorobium thiosulfatophilum*, as 100–150 nm-long tubular vesicle structures associated with the cytoplasmic side of the inner membrane [5]. All GSB contain chlorosomes, with either BChl *c*, *d* or *e*, depending on species. Chlorosomes were later discovered in the gliding filamentous bacterium *Chloroflexus* (*Cfx.*) *aurantiacus* [6], a member of the phylogenetically distinct 'filamentous anoxygenic phototrophs' (FAP). In all GSB, chlorosomes are linked to type-1 RC complexes in the cytoplasmic membrane via the BChl *a*-containing FMO protein [7,8]. In contrast, FAP do not contain an FMO protein and their chlorosomes are directly linked to membrane-embedded RC–LH complexes (type-2 RC). Recently,

Abbreviations: AFM, atomic force microscopy; BChl(s), bacteriochlorophyll(s); *Ca*, *Chloracidobacterium*; *Cab.*, *Chloroacidobacterium*; *Cba.*, *Chlorobaculum*; *Cfx.*, *Chloroflexus*; EM, electron microscopy; FAP, filamentous anoxygenic phototrophs; FWHM, full width at half maximum; GSB, green sulphur bacteria; LH, light-harvesting; PFT, PeakForce Tapping (AFM); QNM, Quantitative Nanomechanical Mapping; RC, Reaction Centre; TEM, transmission electron microscopy; TM, Tapping Mode (AFM); 2-D, two-dimensional; 3-D, three-dimensional

* Corresponding author. Tel.: +44 114 222 4191; fax: +44 114 222 2711.
E-mail address: c.n.hunter@sheffield.ac.uk (C.N. Hunter).

0005-2728/$ – see front matter.
http://dx.doi.org/10.1016/j.bbabio.2013.07.004

Bryant and co-workers [24] discovered a chlorosome-containing organism, named "*Candidatus Chloracidobacterium thermophilum*," (hereafter *Ca.* C. thermophilum) which belongs to the phylum Acidobacteria. This represents the first example of a new phylum for bacterial phototrophs for many years. It contains unusual type-1 RCs [9] and a novel FMO protein [10,11]. The photosynthetic apparatus of this unique photoheterotroph is beginning to be characterised [12–14].

A single *Chlorobaculum* (*Cba.*) *tepidum* chlorosome is estimated to contain 200,000–250,000 BChl *c*, 2500 BChl *a*, 20,000 carotenoids, 18,000 quinones and 5000 proteins, bounded by a lipid monolayer of 20,000 lipids [15]. Chlorosomes can be isolated by sucrose gradient centrifugation of cell extracts and are highly stable when prepared in the presence of sodium thiocyanate [16]. Chlorosome size varies depending on species. Size also increases during chlorosome development [17] and can vary with growth conditions, such as light intensity [18].

The part of the chlorosome envelope that attaches to the cytoplasmic membrane is named the 'baseplate', which was first observed in freeze-fracture images as a flat, paracrystalline protein array [19,20]. The baseplate protein, CsmA, contains BChl *a* and has been characterised in *Cfx. aurantiacus* and *Cba. tepidum* [21,22] and the gene for *csmA* has also been found in *Cfx. aurantiacus* [23] and *Ca.* C. thermophilum [24]. The baseplate was recently visualised by cryo-electron microscopy (cryo EM), confirming that it is only found on one face of the chlorosome. Consistent with cross-linking studies and modelling of the NMR structure [25], the cryo-EM studies suggested that the baseplate is built up from CsmA dimers [26]. The baseplate attaches to FMO in GSB, or directly to the cytoplasmic membrane in FAP and models have been constructed [25].

BChl molecules in chlorosomes were originally predicted to stack end-to-end forming rods and filaments, similar to the 'J-aggregates' of self-assembling dyes [27], explaining the red shift of the BChl *c* Q_y absorption maxima to ~750 nm as observed for the native aggregated state in chlorosomes. Early studies by freeze-fracture electron microscopy suggested that the BChl molecules in chlorosomes formed tubular structures [19,20], and similar suggestions were subsequently advanced by Holzwarth and co-workers [3,28]. Pšenčík and co-workers were the first to suggest an alternative structure, described as "undulating lamellae," which were purported to explain results obtained from cryo-electron microscopy and X-ray diffraction analyses [29,26]. More recently, a combination of systems biology, cryo-electron microscopy, solid-state NMR, and molecular modelling led to structures for BChl *c* and *d* in chlorosomes of *Cba. tepidum*. These studies have conclusively established that the BChls in these chlorosomes form concentric coaxial nanotubes [30]. The tetrapyrrole head groups form surfaces that are stabilized by interactions between the hydrophobic tails of the BChls, which form bilayers in the interior and which are capped by the tails of glycolipids within the chlorosome envelope.

Given the structural and functional differences between the chlorosomes of GSB and FAP, and the recent discovery of *Ca.* Cab. thermophilum [24], we undertook a three-way ultrastructural comparison of chlorosomes from *Cba. tepidum*, *Cfx. aurantiacus* and *Ca.* C. thermophilum using transmission EM (TEM) and atomic force microscopy (AFM), and we compared the emission properties of single chlorosomes from each bacterium using fluorescence microscopy. The ability of AFM to image nanoscale structures under liquid and nearly native conditions has enabled the first imaging of chlorosomes anchored to the cytoplasmic membrane.

2. Materials and methods

2.1. Cell growth and purification of chlorosomes

Chlorosomes were isolated from cells of *Ca.* C. thermophilum as described by Garcia Costas et al. [12]. To isolate cell membranes with attached chlorosomes, cells were broken as described by Garcia Costas et al. [12] but in the absence of 2.0 M sodium thiocyanate. After a low-speed centrifugation to remove unbroken cells and large cell debris, membranes with bound chlorosomes were pelleted by centrifugation and resuspended in 10 mM K-phosphate buffer, pH 7.5, containing 150 mM NaCl.

Chlorosomes from *Cba. tepidum* and *Cfx. aurantiacus* were isolated using a modified method of Feick et al. [31]. Whole cells were disrupted using a Branson Sonifier and the suspension was centrifuged at 16,000 ×*g* for 20 min. The supernatant was centrifuged at 225,000 ×*g* for 2 h at 4 °C. The pellet containing whole membranes was resuspended in 20 mM Tris–HCl pH 8 and homogenized using an overhead stirrer with a Teflon mixer. Concentrated whole membranes were diluted and mixed to a final concentration of $OD_{865\ nm}$ = 2–4 cm^{-1} for *Cfx.* and $OD_{745\ nm}$ = 50 cm^{-1} for *Cba. tepidum* in 2 M NaI and 20 mM Tris, pH 8. The mixture was briefly sonicated, then ultracentrifuged for 16 h at 135,000 ×*g*, at 4 °C. This yielded a floating pellet enriched in chlorosomes whilst the supernatant contained mostly membranes. The floating pellets were pooled and resuspended in 20 mM Tris–HCl (pH 8). These partially purified chlorosomes were layered onto a two-step (20/40%, wt./vol.) sucrose gradient in 20 mM Tris–HCl, pH 8 and centrifuged at 135,000 ×*g* for 16 h at 4 °C. Purified chlorosomes banded at the interface of the gradient layers and pure chlorosomes were collected from the top of the band whilst membranes still contaminated the lower part of the band. To reduce the possibility of membrane contamination further, the top band was subjected to a second sucrose gradient after diluting with one volume of 20 mM Tris (pH 8). The final chlorosome stock was in ~20% (wt./vol.) sucrose, 20 mM Tris pH 8.0 and frozen at −80 °C until use.

2.2. Transmission electron microscopy (TEM)

Chlorosomes were applied to glow-discharged carbon-coated copper grids and stained with 0.75% (w/v) uranyl formate. Images were recorded at 100 kV on a Philips CM100 microscope equipped with a Gatan Ultrascan 667 CCD camera at magnifications between ×8900 and ×28,500. Images were analysed using Digital Micrograph software (Gatan, Inc.).

2.3. Atomic force microscopy (AFM)

Chlorosomes were diluted to an absorbance of approximately 0.1 at the BChl *c* Q_y peak in 10 mM HEPES, 150 mM potassium chloride, and 25 mM magnesium chloride (pH 7.5), adsorbed for 1 h onto freshly cleaved mica (Agar Scientific). They were then exchanged into an imaging buffer of 10 mM HEPES and 100 mM potassium chloride (pH 7.5). Tapping Mode AFM (TM-AFM) was carried out using a Multimode microscope with a NanoScope IV; PeakForce Tapping mode AFM (PFT-AFM) (proprietary imaging mode, Bruker Nano Surfaces Business, formerly Veeco Instruments Ltd) was carried out using a Multimode VIII system, both equipped with an 'E' scanner (15 × 15 μm) (Bruker). Sharpened SiN probes (k = 0.15 N m^{-1}) (TR800PSA, Olympus) were used for standard TM-AFM, operating at frequencies between 7 and 9 kHz. For PFT-AFM, BioLever mini 'AC40TS' probes (ultra-small rectangular cantilever, k = 0.10 N m^{-1}) as they combine a soft cantilever with a higher resonant frequency, more amenable to the 2 kHz approach/withdraw ramp cycle. Parameters were optimised whilst imaging, to minimise forces exerted on the sample. Images were recorded (512 × 512 pixels) at scan frequencies of 0.5–1.5 Hz. Topographs were 'flattened' and images generated using NanoScope Analysis software (v1.20). Height profile analysis was performed using Gwyddion software (open source, v2.20) by careful measurement of height profiles across individual chlorosomes.

To estimate the dimensions of chlorosomes using AFM, height profiles were measured across the long axis and short axis of individual

chlorosomes. From these profiles, the maximum *height* of the chlorosome above the mica surface was measured. *Length* and *width* were measured from the profiles across the long axis and short axis, respectively, as full width at half maximum (FWHM). This is thought to take account of known AFM tip convolution effects and to allow a fair and reproducible comparison of samples [32]. *Volume* (*V*) was calculated from the dimensions measured by modelling chlorosomes as ellipsoids, using the formula: "$V = 4/3\ \pi\ abc$" (where *a*, *b*, *c* = ellipsoidal radii, i.e. *length*/2, *width*/2 and *height*/2).

2.4. Fluorescence microscopy

Samples were adsorbed onto specially cleaned and chemically treated glass Petri dishes, prepared as follows. Each glass bottom dish (from WillCo wells BV, GWSt-5040) was cleaned by incubation for 2 h in a 1:20 mixture of 100% ethanol and 15 M sodium hydroxide. The clean dishes were then extensively washed with water and dried with N_2 gas; 0.01% (w/v) poly-L-lysine was then added into each dish for at least 2 h. Immediately prior to usage, the dishes were again washed extensively with water, dried with N_2 gas, and the sample was added. Chlorosomes were diluted to an absorbance of approximately 0.02 at the BChl *c* Q_y peak using fluorescence buffer (20 mM HEPES, 25 mM sodium dithionite, pH 7.5) and adsorbed onto the dishes for 30–60 min, washed in the same buffer and then imaged.

The custom-built microscope set-up consisted of an Axio Observer A1 inverted optical microscope (Carl Zeiss Ltd.), combined with a BioScope Catalyst AFM with a NanoScope 8 Controller (Bruker Nano Surfaces Business, formerly Veeco Instruments Ltd). For fluorescence imaging a solid state laser (473 nm), which was then expanded so that it completely filled the aperture of the oil immersion lens (63×, NA 1.42), allowed us to get a tightly focused laser spot with a diameter of approximately 400 nm. The sample was then raster-scanned using the AFM x–y scan stage across this laser spot. The fluorescence signal was acquired through a 550 nm longpass filter using an avalanche photodiode detector (Perkin-Elmer) synchronised with the raster-scan of the sample so that the total number of photons was counted for each image pixel. The photodetector signal was digitised and then fed into the AFM NanoScope software to generate a fluorescence image. Alternatively, the fluorescence signal could be sent to a monochromator and an EM CCD camera (Princeton Instruments) in order to acquire spectra at a defined position. In this case the data was acquired using LightField software (Princeton Instruments). To achieve sufficient signal-to-noise for single particle analysis, at least 20 spectra (each with 1000 ms exposure) were usually acquired for each chlorosome. These spectra were averaged and analysed using Origin graphical software (v7.5, OriginLab Corporation).

3. Results

3.1. Comparative overview of three different types of chlorosomes

Chlorosomes were purified from photosynthetically grown cultures by sucrose gradient centrifugation of cell extracts, as described in Section 2.1, from *Cfx. aurantiacus*, *Cba. tepidum* and *Ca.* C. thermophilum. The absence of significant 675 nm absorption peaks arising from monomeric BChl indicated that these chlorosome preparations were intact (Fig. 1). The absorption spectra of chlorosomes from *Cfx. aurantiacus* and *Ca.* C. thermophilum were very similar, with major absorption peaks for the BChl *c* aggregates in vivo occurring at 462 nm (Soret band) and 742 or 743 nm (Q_y transition). The chlorosomes from *Cba. tepidum* had slightly red-shifted absorption maxima at 457 nm and 747 nm, and Q_y transition peak for the BChl *c* aggregates was broader. A minor absorption peak at 800 nm was observable in chlorosomes of *Cfx. aurantiacus* and *Ca.* C. thermophilum, which arises from the BChl *a* associated with CsmA in the chlorosome baseplate.

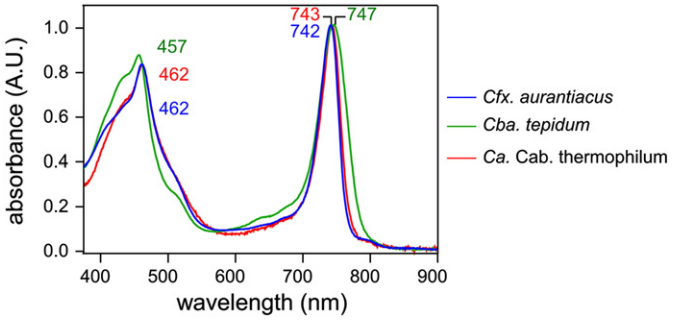

Fig. 1. Absorbance spectra of chlorosomes. Room temperature absorbance spectra of the chlorosome samples, as labelled in the figure. Wavelength of BChl *c* maxima shown.

This absorbance band is masked by the broader Q_y peak in *Cba. tepidum*. These absorption spectra are consistent with previous reports; the minor differences among these samples and previous reports for similar chlorosome preparations arise from minor differences in the BChl *c* homolog composition of specific samples, which in turn produce slight differences in the site energies of the BChl *c* molecules in the chlorosomes isolated from different organisms and cultures [1,24].

The chlorosomes were initially compared by transmission electron microscopy (TEM) of negatively stained samples to give an overview of chlorosome sizes and to check their purity (Fig. 2). This technique has good lateral resolution but images are two-dimensional and provide no height information. All chlorosomes appeared as roughly 'oblong' structures with approximate dimensions (100–200) × (30–60) nm, and seemed to be relatively homogeneous with no other unexpected structures. The chlorosomes of *Cba. tepidum* appeared larger than those of *Ca.* C. thermophilum and *Cfx. aurantiacus*, which were similar in size. The contrast on the surface of the chlorosomes of *Ca.* C. thermophilum was suggestive of a somewhat undulating surface, as previously reported [3,12].

The chlorosomes were then compared using PeakForce Tapping mode AFM (PFT-AFM) under liquid at room temperature (Fig. 3). This three-dimensional mapping showed that the chlorosomes are ellipsoids of variable size. 3-D rendering of the AFM data showed that the surfaces of the chlorosomes were not smooth, but had bumps and undulations that differed among individual chlorosomes (Fig. 3B). Thus, no two chlorosomes are the same with respect to size, shape or surface contours. It was found that PFT-AFM was more effective than standard Tapping Mode (TM) AFM for these samples. In PFT-AFM force curves are generated at each pixel and the maximum force applied to the sample, the 'peak force', is closely controlled. Real-time analysis of the force curve data yields measurements for the height, amplitude-error and, using the Quantitative Nanomechanical Mapping (QNM) module, various mechanical properties. Whereas TM-AFM would often displace chlorosomes, moving/pushing them across the mica substrate and making imaging inaccurate (data not shown), PFT-AFM allowed accurate tracking of all chlorosomes with very good correspondence of the trace and retrace signals. Although it was not a focus of this study, by imparting sequentially increasing forces during imaging, chlorosomes could be deformed in a controlled manner, with sequential decrease in the imaged height and a related increase in the deformation signal until their destruction begins at peak forces of 1200 pN (for example Fig. S1, *Cba. tepidum* sample, bottom right panel). In comparison, significant deformation of membrane vesicles from the purple phototrophic bacterium *Rhodobacter sphaeroides* was observed at forces above 600 pN. By using a peak force of ~100 pN for chlorosomes, accurate height measurements could be made on chlorosomes in their native form in buffered solution (Fig. 3).

The dimensions of the three types of chlorosomes measured by PFT-AFM were analysed (Table 1). Additionally, these results were

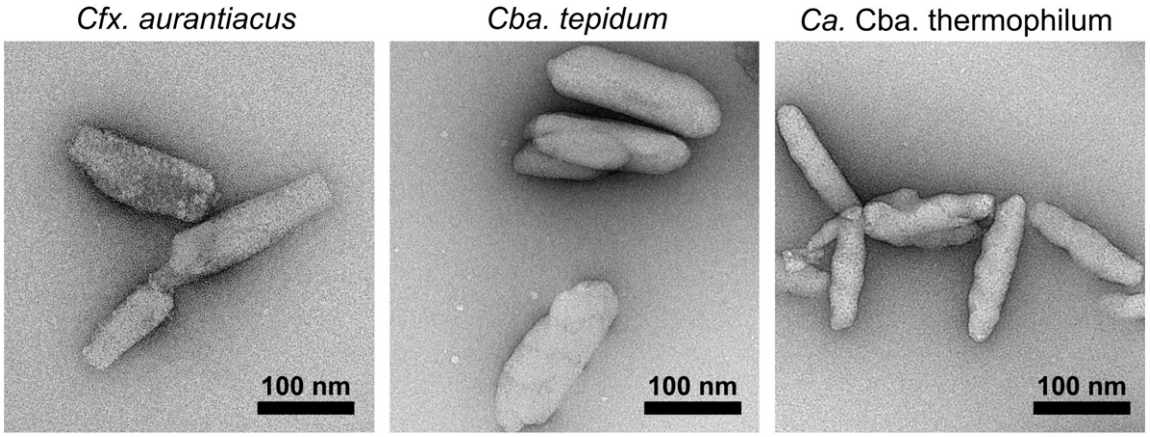

Fig. 2. Overview of chlorosomes by TEM. Transmission electron microscopy of negatively-stained chlorosomes, from the species as labelled. Low magnification (upper row) and higher magnification (lower row).

compared with those for chlorosomes from *Cba. tepidum* that had been dried onto mica and imaged in air, to align our measurements made under fluid with previous studies in which AFM was performed in air. Full width at half maximum (FWHM) measurements were made for length and width, which is thought to take account of known AFM tip convolution imaging artefacts and allow a fair comparison [32]. The chlorosome volume was then calculated from the dimensions measured, modelling a chlorosome as an ellipsoid, as in previous studies [33,34]. Chlorosomes from *Cba. tepidum* were the largest (133 × 57 × 36 nm; 141,000 nm^3 volume), and had significantly greater width and height and slightly greater length than chlorosomes from *Cfx. aurantiacus* (120 × 44 × 30 nm, 84,000 nm^3 volume). Chlorosomes from *Ca.* C. thermophilum were found to be shorter and slightly narrower (99 × 40 × 31 nm; 65,000 nm^3 volume) than those of *Cfx. aurantiacus*. Dried chlorosomes from *Cba. tepidum*, imaged in air, had significantly lower height and smaller volume compared to their hydrated counterparts, confirming that chlorosomes shrink after dehydration, and underlining the importance of imaging biological samples under hydrated conditions (in buffers). AFM has sub-nanometre vertical resolution and a lateral resolution of a few nanometres, related to the sharpness of the probe's silicon tip, which makes the accuracy of our lateral measurements comparable to TEM, but with the advantage of a highly accurate third dimension of height. For each organism tested here, there was a significant range in the size of chlorosomes within each population reflected in the relatively high S.D. values reported in Table 1. With

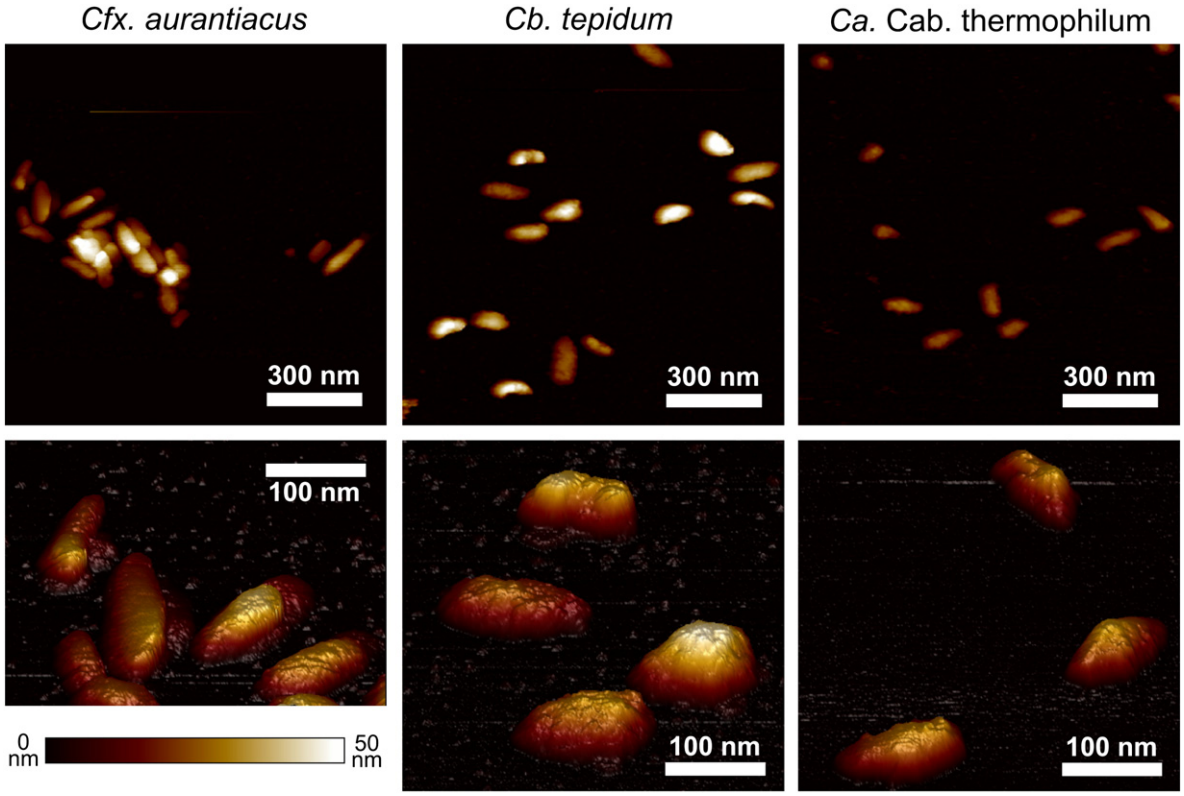

Fig. 3. Overview of chlorosomes by PeakForce Tapping AFM. Atomic force microscopy (PeakForce Tapping mode) of chlorosomes on mica, in fluid. All topographs are to equal z-scale (bar, bottom-left). Top row: Low magnification topographs Bottom row: Higher magnification topographs, data displayed in 3-D.

Table 1
Analysis of chlorosome dimensions for different species. Analysis of AFM topographs of the three chlorosome samples (Figure 3 and further topographs, not shown). Length and width were measured from height profiles across the long axis and short axis (respectively) of individual chlorosomes, as full width at half maximum (FWHM) measurements from the sections, to allow reproducible comparisons taking into account imaging artefacts due to tip geometry. Height was the maximal height from the mica substrate. Volume was calculated from the dimensions measured, modelling chlorosomes as ellipsoids, using the formula: $V = \frac{4}{3}\pi abc$ (where a, b, c = ellipsoidal radii, which here is length/2, width/2 and height/2).

Chlorosome species	Measured (nm) (±S.D.)			Volume (±S.D.)
(n = number measured)	Length	Width	Height	($\times 10^3$ nm^3)
[a]*Cfx. aurantiacus* (n = 7)	120 (±20)	44 (±8)	30 (±4)	84 (±27)
[a]*Cba. tepidum* (n = 20)	133 (±28)	57 (±11)	36 (±9)	141 (±44)
[a]*Ca.* C. thermophilum (n = 15)	99 (±15)	40 (±5)	31 (±3)	65 (±13)
[b]*Cba. tepidum* (n = 17)	123 (±34)	51 (±11)	23 (±4)	83 (±47)

[a] Under buffer.
[b] In air.

the accuracy of AFM in mind, it is important to note that the high S.D. values do not reflect inaccurate measurements but a genuine size distribution within each chlorosome population.

3.2. AFM imaging of Ca. C. thermophilum chlorosomes attached to cytoplasmic membranes

The majority of chlorosomes in standard preparations (using sodium thiocyanate) were observed as isolated structures devoid of any attached membranes. Less frequently, chlorosomes appeared to be sitting on top of a sheet-like feature. Fig. 4A–B shows one such example in which two *Ca.* C. thermophilum chlorosomes are observed at the edges of sheet-like features approximately 700 × 300 nm and 5.0–6.8 nm in height. Both 2-D and 3-D representations are shown; for clarity the z-scale was offset to show greatest contrast either at the membrane height range or the chlorosome height range. This sheet is likely to be a segment of the cytoplasmic membrane that is still connected to the chlorosomes. Multiple height levels were observed and height profiles (Fig. 4C) showed that the majority of the patch had a height of ~5.5 nm (*level 2*) with some regions slightly lower (~5.0 nm, *level 1*) and some higher (~6.5 nm, *level 3*). Lipid bilayer membranes can range from 3 to 5 nm in height depending on their lipid composition and phase behaviour [35]; values greater than this are likely to represent protein-containing regions of the membrane. Therefore height levels 1–3 may represent different phases of lipids and protein-containing domains, but the resolution in this image was not sufficient to provide any further detail.

Sodium thiocyanate has been reported to aid detachment of chlorosomes from the cytoplasmic membranes allowing better purification of chlorosomes. Indeed, in chlorosome preparations for which sodium thiocyanate was omitted, TEM images showed many irregular fragments and vesicle-like structures, expected to represent the cytoplasmic membrane, but fewer chlorosomes (Fig. 5A). Higher magnification TEM images (Fig. 5B) of these membranes showed inhomogeneous pooling of stain, which could suggest variations of protein content over the surface of the membrane, but the dehydrated nature of the TEM samples and lack of 3-D information in this technique meant that we were unable to reveal any further detail.

In other membranes for which higher resolution was achieved with AFM, distinct globular protrusions were observed within the membranes (Fig. 6A–B), with a variable separation between features. Fig. 6D shows that these structures were up to 30 nm in width and at a constant height of ~6 nm above the mica surface, confirmed by the multiple height profiles. Further examples of *Ca.* C. thermophilum membranes had a higher density and greater degree of ordering of these globular protrusions (Fig. S2). Features were accurately tracked within each image and the trace and retrace scans were congruent, giving confidence in the data. However, between images the shape

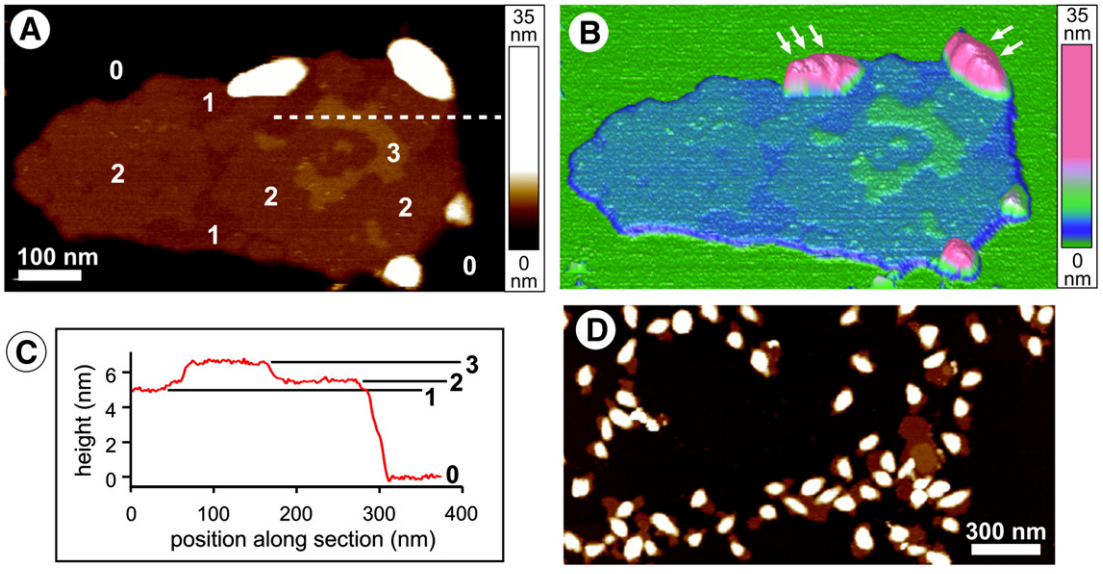

Fig. 4. AFM showing membrane attachment of chlorosomes from *Ca.* C. thermophilum. AFM data showing the rare finding of chlorosomes on top of a membrane sheet from a standard chlorosome preparation for *Ca.* C. thermophilum (A–C). The majority of chlorosomes were associated with membranes in a special chlorosome/membrane preparation for which sodium thiocyanate was omitted (D). A. Topograph showing two chlorosomes that seem to be positioned on top of a membrane with regions at different height levels (regions labelled: 1, 2, 3; mica: 0). The Z-scale is offset to have high contrast between 0–15 nm, the z-scale bar shown. B. 3-D representation of the AFM data in (A). C. Height profile across white dashed-line in (A). Different height levels are denoted as in (A). D. Topograph showing a typical field of chlorosomes and associated membranes from a membrane preparation from *Ca.* C. thermophilum for which sodium thiocyanate was omitted.

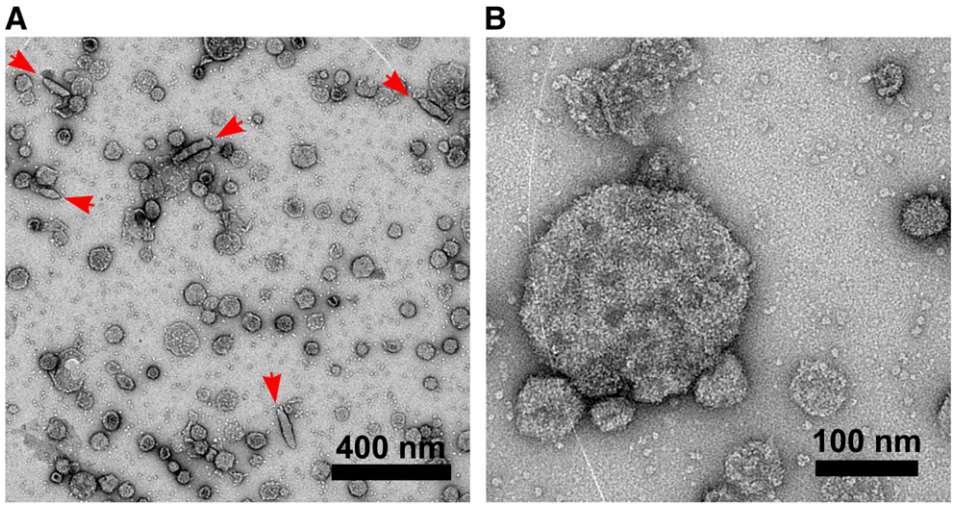

Fig. 5. TEM of a sodium thiocyanate-free preparation of *Ca.* C. thermophilum chlorosomes and membranes. A. Representative TEM image showing potential cytoplasmic membrane fragments and vesicles of irregular shape. Chlorosomes of similar dimensions to those in Fig. 2 are also observed (red arrowheads). B. Higher magnification TEM of membrane fragment showing inhomogeneous pooling of stain.

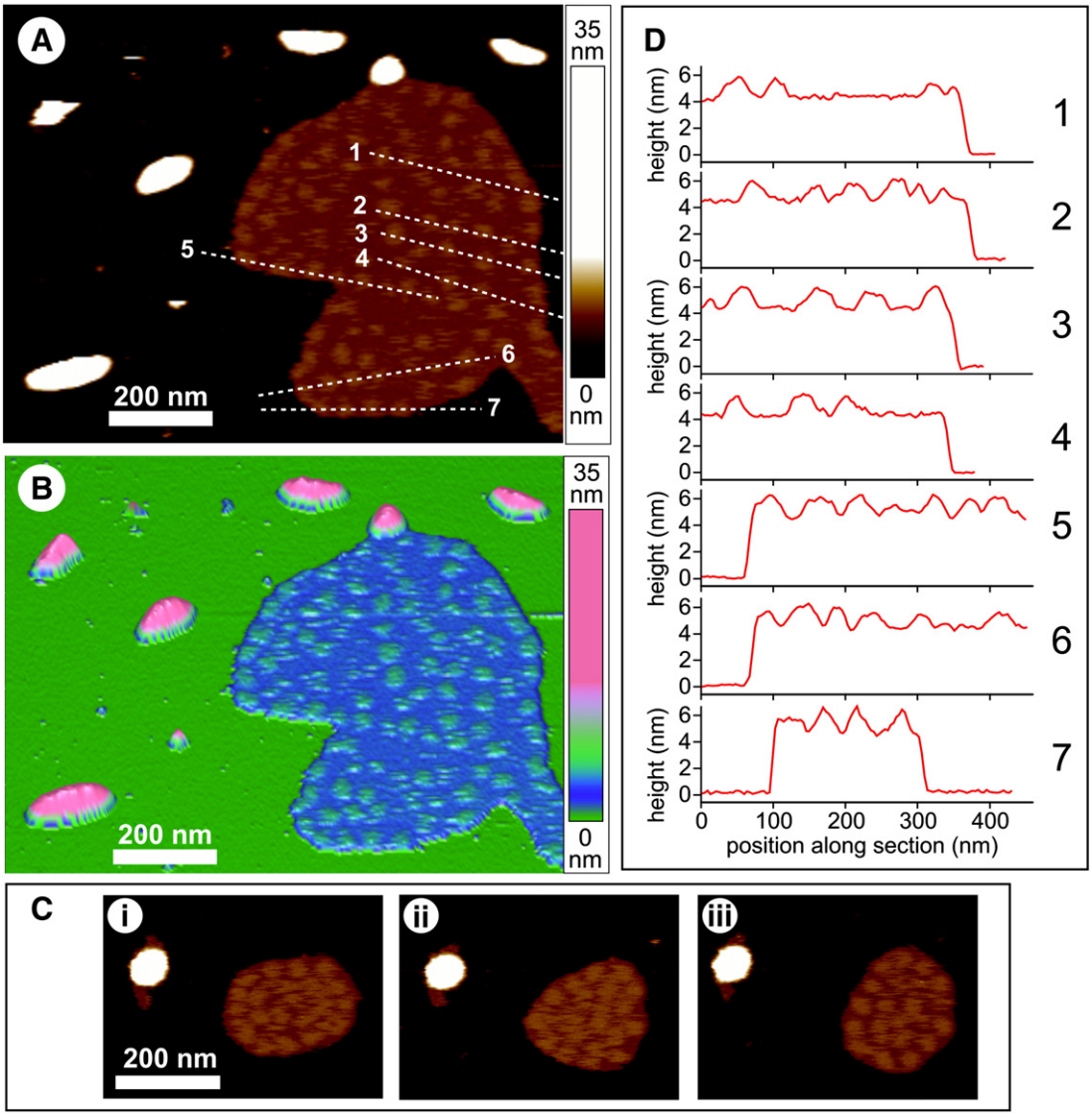

Fig. 6. AFM showing globular protrusions within the *Ca.* C. thermophilum membrane. A. Topograph showing a patch of membrane containing globular protrusions and nearby chlorosomes. The Z-scale is offset to have high contrast between 0–15 nm, the z-scale bar shown. B. 3-D representation of the AFM data in (A). C. A sequence of three consecutive AFM scans showing a patch of membrane with globular protrusions. The membrane patch changes shape between images, suggesting that it has significant fluidity and allowing dynamic changes. D. Height profiles across selected features of interest in the image, at positions indicated by dashed white lines labelled 1–7 in (A).

of each membrane patch and the organisation of the features within it changed. A series of sequential images of another small membrane fragment changing in shape is shown in Fig. 6C. The instability of these membranes suggested that they are fluid at room temperature on the mica surface.

3.3. Spectral imaging of the fluorescence emission properties of individual chlorosomes

Chlorosomes were adsorbed to poly-L-lysine-coated glass Petri dishes and imaged using a custom-built microscope (Section 2.4) under buffer containing sodium dithionite to maintain a reducing environment. A 473 nm laser was used to excite the Soret band of chlorosome BChl *c* aggregates and fluorescence emission was monitored in the near infrared, whilst using a piezo stage to scan the sample in the x–y directions. Fig. 7 (upper panels) shows representative fluorescence images of the three types of chlorosomes, which appear mainly as diffraction-limited spots of 300–400 nm. The resolution was approximately 350 nm, estimated from the closest two spots that could still be defined as separate entities. The similar fluorescence amplitudes indicate that the majority of these spots are likely to arise from single chlorosomes, consistent with the AFM images that showed mostly well-separated chlorosomes at this dilution. Larger, brighter spots indicated that some chlorosomes were closely spaced on the glass surface, as may be expected from a random distribution of particles.

Emission spectra were recorded at positions of interest within the fluorescence image, with the same spatial resolution. Comparison of spectra of individual and small clusters of chlorosomes allowed us to observe differences between individual chlorosomes within a population. Representative spectra from numbered chlorosomes are shown in Fig. 7 (lower panels). Chlorosomes from *Cfx. aurantiacus* had emission maxima which ranged from 747 nm (*spectrum 11*) to 751 nm (*spectrum 5*), with a full-width at half-maximum (FWHM) of ~30 nm. Chlorosomes from *Cba. tepidum* had emission maxima that ranged from 765 nm (*spectrum 8*) to 771 nm (*spectrum 2*), with a FWHM of ~39 nm. Chlorosomes from *Ca.* C. thermophilum had emission maxima that ranged from 749 nm (*spectrum 13*) to 753 nm (*spectrum 7*), with a FWHM of ~28 nm.

4. Discussion

4.1. Chlorosomes from three different phyla of phototrophic bacteria have significantly different dimensions

Widely varying values for the dimensions of chlorosomes have been reported in previous studies, possibly because of the differences and difficulties in sample preparation and analysis regimes. Table 2 compiles the results from some of these measurements for comparison with the data obtained in the study presented here.

The present study undertook a systematic comparison of the dimensions of chlorosome using AFM analysis supported by concomitant TEM examination of the samples. Well-studied chlorosomes from *Cfx. aurantiacus* and *Cba. tepidum* were compared with those from the newly discovered acidobacterium, *Ca.* C. thermophilum. Early AFM studies of chlorosomes either employed carbon coating to provide stability [36,34] or drying onto a surface [37,38,33] to enable the chlorosomes to withstand the high lateral forces of contact mode and tapping-mode AFM imaging. AFM technologies have developed greatly over the last decade and are now more accurate and amenable to imaging soft biological samples under liquid. We employed the relatively new imaging mode of PeakForce Tapping AFM in which the force applied during imaging is minimised by triggering tip retraction at a defined 'peak force'. Whereas standard TM-AFM seemed to

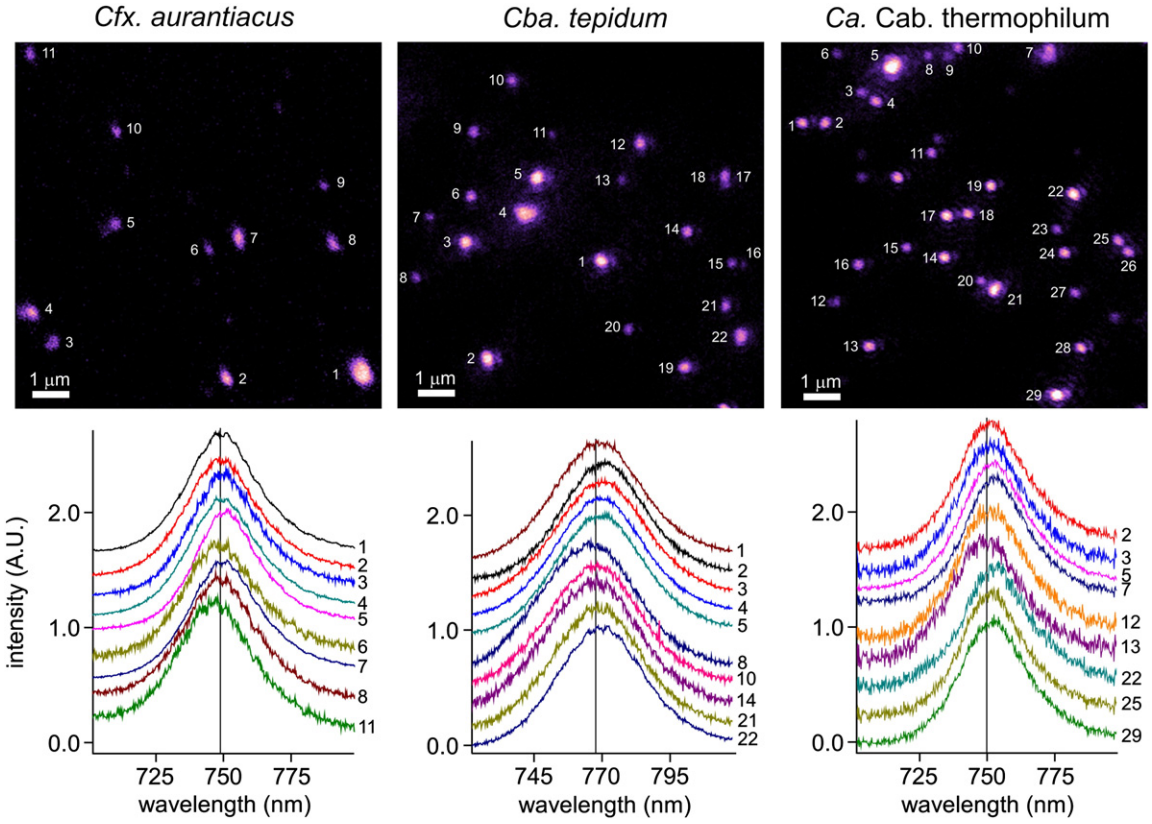

Fig. 7. Heterogeneity in fluorescence emission of individual chlorosomes. The top row shows fluorescence images of single chlorosomes from *Cfx. aurantiacus*, *Cba. tepidum* and *Ca.* C. thermophilum that were collected using a custom-built microscope (see Materials and methods) with 473 nm excitation. The bottom row shows a selection of representative emission spectra collected for these chlorosomes using an EM CCD camera.

Table 2
Comparison of reported dimensions for different chlorosomes.

Species	Sample	Treatment	Technique	Dimensions (nm)			Ratio	Volume	Reference
				L	*W*	*H*	*L*/*W*	($\times 10^3$ nm^3)	
Cfx. aurantiacus[*]	Cells	Thin-sectioned	TEM	~100	50–70	~20	1.7	63[a]	[6]
Cfx. aurantiacus	CHL	Carbon-coated, dried	TM-AFM	99	31	5	3.2	8	[34]
Cfx. aurantiacus	Cells	Freeze-fractured	SEM	106	32	10–20	3.3	27[a]	[18]
Cfx. aurantiacus (5 h)[**]	Cells	Freeze-fractured	SEM	107	39	12	2.7	36	[17]
Cfx. aurantiacus (45 h)[**]	Cells	Freeze-fractured	SEM	135	46	21	2.9	92	[17]
Cfx. aurantiacus	CHL	Dried	TM-AFM	166	97	24	1.7	152	[37]
Cfx. aurantiacus	CHL	Glutaraldehyde, dried	CM-AFM	123	44	11	2.8	64[a]	[38]
Cfx. aurantiacus	CHL	Cryo-frozen	Cryo EM	140–220	30–60	10–20	4.0	64[a]	[26]
Cfx. aurantiacus	CHL	In buffered liquid	PFT-AFM	120	44	30	2.7	84	This study
Cba. tepidum	cells	Thin-sectioned	TEM	100–180	40–60	40–60	2.8	183[a]	[39]
Cba. tepidum	CHL	Dried	TM-AFM	194	104	26	1.9	165	[37]
Cba. tepidum	CHL	Dried	TM-AFM	174	91	11	1.9	91	[33]
Cba. tepidum	CHL	Cryo-frozen	Cryo EM	140–180	~50	–	1.7	–	[29]
Cba. tepidum	CHL	(Unknown)	AFM[#]	212	122	35	1.7	474[a]	[50]
Cba. tepidum	CHL	In buffered liquid	PFT-AFM	133	57	36	2.3	141	This study
Ca. C. thermophilum	CHL	Dried, stained	TEM	100	31	31	3.2	50[a]	[12]
Ca. C. thermophilum	CHL	In buffered liquid	PFT-AFM	99	40	31	2.5	65	This study

Comparison of the dimensions reported for chlorosomes in different species using different techniques. Dimensions, *L*, *W*, *H* (*length*, *width* and *height*) all rounded to the nearest integer for comparability. Volume (in 1000s nm^3), as reported in the studies (without superscript) or where no value is quoted (superscript 'a') calculated from the *L*, *W* and *H* values, using the formula $V = 4/3\ \pi\ abc$ (where *a*, *b*, *c* = ellipsoidal radii, *L*/2, *W*/2 and *H*/2), all rounded to the nearest 1000 for comparability.
'CHL', in the 'sample' column, means 'purified chlorosomes', as opposed to fractured or sectioned cells. 'SEM', scanning EM; 'TEM', transmission EM. 'TM-AFM', tapping mode AFM; 'CM-AFM', contact mode AFM; 'PFT-AFM', PeakForce Tapping AFM.
[*]Values for the 'wide' *OH-64-fl* and *OK-70-fl* strains reported in this study.
[**]Values for cells at different periods after transfer from chemotrophic (t = 0 h) to phototrophic conditions.
[#]No details given about the mode of AFM used or imaging conditions in this study.

displace chlorosomes from the mica support during imaging, PFT-AFM did not cause any noticeable movement of the features being imaged, resulting in accurate tracking of chlorosomes under liquids.

Previous studies had suggested that AFM of dried chlorosomes underestimates their native heights [33] and our PFT-AFM imaging confirms this: the height of dried chlorosomes from *Cba. tepidum* imaged in air is significantly lower (23 ± 4 nm) than hydrated chlorosomes (36 ± 9 nm) imaged in liquid (Table 1). This emphasizes the importance of imaging chlorosomes in their native, hydrated form without staining, freezing or drying. PFT-AFM measured the native dimensions of the chlorosomes in 3-D, finding that those from *Cba. tepidum* were largest (especially in width), *Cfx. aurantiacus* chlorosomes were intermediate in size and that chlorosomes from *Ca.* C. thermophilum were smallest (Fig. 3, Table 1). This trend is consistent with the results from the 2-D data for negatively stained chlorosomes examined by TEM (Fig. 2) and is also consistent with previous studies that found that chlorosomes from *Cba. tepidum* are generally larger than chlorosomes from *Cfx. aurantiacus* [39]. The absolute values we measured for chlorosome length and width are in broad agreement with previous TEM and AFM measurements (Table 2). Chlorosome heights measured here were generally slightly greater than those found in the majority of previously published studies. This arises from imaging under liquid at room temperature and might also arise from the sub-nanometre accuracy of AFM.

With regard to possible effects of adsorption to the substrate on chlorosomes, light-harvesting membrane protein complexes have been imaged with AFM to high resolution for many years and the mica surface does not seem to cause any significant disruption to native structures [40,41]. Likewise we do not expect surface adsorption, which is likely to involve nonspecific ionic interactions between the negatively charged mica, cations in the buffer solution and the charged groups on the exterior of chlorosomes, to cause any major rearrangements of chlorosome structure. Fig. S1 shows that *Cba. tepidum* and *Cfx. aurantiacus* chlorosomes are relatively robust and resist mechanical deformation by forces up to 1000 pN, so adverse effects of surface adsorption appear to be unlikely. We expect that chlorosomes usually adsorb baseplate side-down onto mica as chlorosomes are potentially flatter on this side and also because we would have expected to visualise the periodicity of the baseplate CsmA array if it was exposed 'face-up' to the AFM tip.

We found that whilst chlorosomes from each species had a characteristic mean there was a significant size distribution, reflected in the standard deviations of approximately 20%. Similarly wide ranges in chlorosome dimensions have been previously observed with AFM and EM of purified chlorosomes and chlorosomes within cell sections (see references in Table 2). Given the accuracy of AFM, the range we observe in chlorosome dimensions represents genuine differences in the size of chlorosomes within a population of cells. We expect that whilst cells growing under specific growth conditions may have an optimal chlorosome size, not all chlorosomes will reach these proportions. Size has been shown to increase during chlorosome development [17] and because cells within one culture do not grow and divide in synchrony our measurements represent chlorosomes at different degrees of maturity.

The reasons behind differences in the dimensions of chlorosomes from different phyla of phototrophic bacteria are unclear and probably reflect physiological differences relating to the adaptation of each organism to specific ecological niches. For example, *Cfx. aurantiacus* and *Ca.* C. thermophilum occur in the microbial mats associated with hot springs in Yellowstone National Park, where light intensities can reach quite high values [24,42]. This controlled size analysis of *Ca.* C. thermophilum chlorosomes by AFM allows the first detailed comparison with chlorosomes from other bacteria. Differences in chlorosome size could also simply reflect differences in culture growth conditions [18]. It is known that proteins of the chlorosome envelope influence the size and shape of chlorosomes [42,43], and the protein compositions of the chlorosome envelopes of these three organisms are quite different [44]. Similarly, differences in the distribution of BChl *c* homologs in chlorosomes also can modify the size and shape of chlorosomes [45].

The application of the QNM mode of AFM provided a deeper level of analysis of chlorosome structure, and examination of the mechanical properties of *Cba. tepidum* and *Cfx. aurantiacus* chlorosomes shows that relatively high peak forces of 1000–2000 pN are required to disrupt the integrity of these structures (Fig. S1). In comparison, well-characterised membrane vesicles from the purple phototrophic

bacterium *Rba. sphaeroides* [46] could be compressed at 600 pN and were completely disrupted at higher forces. This can be compared with the 100–200 pN forces required to extract the transmembrane helices of bacteriorhodopsin from the purple membrane [47]. The fact that the chlorosomes seem to be less compressible and more difficult to disrupt suggests that the tight packing of pigments inside the chlorosome lends a degree of mechanical stability to these structures. The thousands of pigment–pigment stacking interactions confer stability to these supramolecular assemblies, collectively underpinning the structure and function of the chlorosome.

4.2. Observation of chlorosomes attached to their native cytoplasmic membrane

Chlorosomes still attached to cytoplasmic membranes were observed by AFM (see Figs. 4, 6 and S2). Membrane-associated chlorosomes were uncommon in a standard preparation of purified chlorosomes, but almost all chlorosomes were associated with membranes in preparations in which sodium thiocyanate was omitted. The attached membranes were observed to have different domains with distinct heights, which presumably represent different protein domains, although resolution was limited. In *Ca.* C. thermophilum preparations, distinct globular protrusions, up to 30 nm wide and 6 nm in height, were observed. The fact that the membrane patches changed shape, and that the protein features seem to be dynamic, suggest either that the membranes are rich in fluid phase lipids allowing greater mobility than protein-packed domains, or that these features are weakly attached to their membranes and easily disrupted by the AFM probe. These membrane features are intriguing and their presence in preparations with chlorosomes could suggest that they relate to the chlorosomes in some way, but it is challenging to identify these features with either TEM or AFM alone, limited by resolution and the lack of chemical identification.

The imaging of chlorosomes attached to membranes, directly observed under native conditions, is consistent with these membrane-extrinsic light-harvesting structures funnelling absorbed solar energy to membrane-bound reaction centres where photochemistry is performed. These images show that there is considerable potential for using AFM for interrogation of chlorosomes still associated with their native cytoplasmic membranes, a state that is as close to in vivo conditions as possible. Furthermore the novel protrusions in the cytoplasmic membrane are seen for the first time and their distribution, size and height have been recorded. The size of these membrane features corresponds to the chlorosome width (~30 nm); perhaps they represent clusters of the membrane-associated *Ca.* C. thermophilum FMO protein [10,11]. The fluid nature of these membranes, revealed in Fig. 6C, would suggest that membrane-attached chlorosomes have some lateral mobility but data would be needed to test this idea. Future studies of more highly purified cytoplasmic membranes or reconstituted proteins/lipids of known composition could reveal the definitive nature of these protrusions.

4.3. Chlorosomes show some heterogeneity in their fluorescence emission characteristics

Several previous studies have used fluorescence microscopy and spectroscopy to investigate single chlorosomes from *Cba. tepidum* and *Cfx. aurantiacus* [36,48,49]. The authors reported significant heterogeneity in the position of fluorescence emission peaks for chlorosomes from both species [49]. In the current study, we have compared chlorosomes from the recently discovered acidobacterium *Ca.* C. thermophilum with chlorosomes from *Cba. tepidum* and *Cfx. aurantiacus* (Fig. 7). We found that within each type of chlorosome there was a small but significant degree of heterogeneity in the fluorescence emission maxima, with chlorosomes of *Cba. tepidum* having the greatest range, as well as largest full-width half maximal value. Our data for *Cba. tepidum* and *Cfx. aurantiacus* chlorosomes are in agreement with the previous studies [49] and the first such measurements on *Ca.* C. thermophilum chlorosomes allow us to compare the physical and spectral characteristics of chlorosomes from three different phyla. In previous studies [36,48,49] the authors attributed the spectral heterogeneity of *Cba. tepidum* and *Cfx. aurantiacus* chlorosomes to the variable distribution between individual chlorosomes of BChl *c* homologs, which have subtle differences in their absorbance and fluorescence spectra. *Ca.* C. thermophilum has been reported to contain multiple BChl *c* homologs with different alkylation and alcohol esterifications to the chlorin ring [24], so it is likely that the same explanation of spectral heterogeneity applies. It seems that a heterogeneous distribution of BChl *c* homologs is a general feature of chlorosomes. Another cause of the spectral heterogeneity within each type of chlorosome could be the varying sizes and shapes apparent in the 3-D rendered AFM images (Fig. 3). These variations could reflect differences in the internal suprastructural arrangements of the stacked BChls within each chlorosome, also observed in cryo-EM analyses of individual chlorosomes [28].

Supplementary data to this article can be found online at http://dx.doi.org/10.1016/j.bbabio.2013.07.004.

Acknowledgements

C.N.H. acknowledges financial support from the Biotechnology and Biological Sciences Research Council (UK). P.G.A. was supported by a doctoral studentship from the Biotechnology and Biological Sciences Research Council (UK). This work was supported as part of the Photosynthetic Antenna Research Center (PARC), an Energy Frontier Research Center funded by the U.S. Department of Energy, Office of Science, Office of Basic Energy Sciences under Award Number DE-SC 0001035. PARC's role was to partially fund the Multimode VIII AFM system and to provide partial support for J.W. and C.N.H. Work performed in the laboratory of D.A.B. was funded by grant DE-FG02-94ER20137 from the U.S. Department of Energy. A.J.C. was funded by the EPSRC grant EP/E059716/1; B.R. was funded through an EPSRC doctoral training award.

References

[1] R.E. Blankenship, K. Matsuura, Antenna complexes from green photosynthetic bacteria, in: B.R. Green, W.W. Parson (Eds.), Light-harvesting Antennas, Kluwer Academic Publishers, Dordrecht, 2003, pp. 195–217.
[2] N.U. Frigaard, D.A. Bryant, Seeing green bacteria in a new light: genomics-enabled studies of the photosynthetic apparatus in green sulfur bacteria and filamentous anoxygenic phototrophic bacteria, Arch. Microbiol. 182 (2004) 265–276.
[3] G.T. Oostergetel, H. van Amerongen, E.J. Boekema, The chlorosome: a prototype for efficient light harvesting in photosynthesis, Photosynth. Res. 104 (2010) 245–255.
[4] D.A. Bryant, N.U. Frigaard, Prokaryotic photosynthesis and phototrophy illuminated, Trends Microbiol. 14 (2006) 488–496.
[5] G. Cohen-Bazire, N. Pfennig, R. Kunisawa, The fine structure of green bacteria, J. Cell Biol. 22 (1964) 207–225.
[6] B.K. Pierson, R.W. Castenholz, A phototrophic gliding filamentous bacterium of hot springs, *Chloroflexus aurantiacus*, gen. and sp. nov, Arch. Microbiol. 100 (1974) 5–24.
[7] R.E. Blankenship, J.M. Olson, M. Miller, Antenna complexes from green photosynthetic bacteria, in: R.E. Blankenship, M.T. Madigan, C.E. Bauer (Eds.), Anoxygenic Photosynthetic Bacteria, Kluwer Academic Publishers, The Netherlands, 1995, pp. 399–471.
[8] Y.F. Li, W.L. Zhou, R.E. Blankenship, J.P. Allen, Crystal structure of the bacteriochlorophyll *a* protein from *Chlorobium tepidum*, J. Mol. Biol. 271 (1997) 456–471.
[9] Y. Tsukatani, S.P. Romberger, J.H. Golbeck, D.A. Bryant, Isolation and characterization of homodimeric type-I reaction center complex from *Candidatus Chloracidobacterium thermophilum*, an aerobic chlorophototroph, J. Biol. Chem. 287 (2012) 5720–5732.
[10] Y. Tsukatani, J. Wen, R.E. Blankenship, D.A. Bryant, Characterization of the FMO protein from the aerobic chlorophototroph, *Candidatus Chloracidobacterium thermophilum*, Photosynth. Res. 104 (2010) 201–209.
[11] J. Wen, Y. Tsukatani, W. Cui, H. Zhang, M.L. Gross, D.A. Bryant, R.E. Blankenship, Structural model and spectroscopic characteristics of the FMO antenna protein from the aerobic chlorophototroph, *Candidatus Chloracidobacterium thermophilum*, Biochim. Biophys. Acta Bioenerg. 1807 (2011) 157–164.
[12] A.M. Garcia Costas, Y. Tsukatani, S.P. Romberger, G.T. Oostergetel, E.J. Boekema, J.H. Golbeck, D.A. Bryant, Ultrastructural analysis and identification of envelope proteins

of "*Candidatus Chloracidobacterium thermophilum*" chlorosomes, J. Bacteriol. 193 (2011) 6701–6711.
[13] A.M. Garcia Costas, Y. Tsukatani, W.I. Rijpstra, S. Schouten, P.V. Welander, R.E. Summons, D.A. Bryant, Identification of the bacteriochlorophylls, carotenoids, quinones, lipids, and hopanoids of "*Candidatus Chloracidobacterium thermophilum*", J. Bacteriol. 194 (2012) 1158–1168.
[14] A.M. Garcia Costas, Z. Liu, L.P. Tomsho, S.C. Schuster, D.M. Ward, D.A. Bryant, Complete genome of *Candidatus Chloracidobacterium thermophilum*, a chlorophyll-based photoheterotroph belonging to the phylum Acidobacteria, Environ. Microbiol. 14 (2012) 177–190.
[15] N.U. Frigaard, J.A. Maresca, C.E. Yunker, A.D. Jones, D.A. Bryant, Genetic manipulation of carotenoid biosynthesis in the green sulfur bacterium *Chlorobium tepidum*, J. Bacteriol. 186 (2004) 5210–5220.
[16] P.D. Gerola, J.M. Olson, A new bacteriochlorophyll *a*-protein complex associated with chlorosomes of green sulfur bacteria, Biochim. Biophys. Acta Bioenerg. 848 (1986) 69–76.
[17] M. Foidl, J.R. Golecki, J. Oelze, Chlorosome development in *Chloroflexus aurantiacus*, Photosynth. Res. 55 (1998) 109–114.
[18] J. Oelze, J. Golecki, Membranes and chlorosomes for green bacteria: structure, composition and development, in: R.E. Blankenship, M.T. Madigan, C.E. Bauer (Eds.), Anoxygenic Photosynthetic Bacteria, Kluwer Academic Publishers, Dordrecht, The Netherlands, 1995, pp. 259–278.
[19] L.A. Staehelin, J.R. Golecki, R.C. Fuller, G. Drews, Visualization of the supramolecular architecture of chlorosomes (chlorobium type vesicles) in freeze-fractured cells of *Chloroflexus aurantiacus*, Arch. Microbiol. 119 (1978) 269–277.
[20] L.A. Staehelin, J.R. Golecki, G. Drews, Supramolecular organization of chlorosomes (chlorobium vesicles) and of their membrane attachment sites in *Chlorobium limicola*, Biochim. Biophys. Acta Bioenerg. 589 (1980) 30–45.
[21] G.A. Montano, H.M. Wu, S. Lin, D.C. Brune, R.E. Blankenship, Isolation and characterization of the B798 light-harvesting baseplate from the chlorosomes of *Chloroflexus aurantiacus*, Biochemistry 42 (2003) 10246–10251.
[22] M.O. Pedersen, J. Underhaug, J. Dittmer, M. Miller, N.C. Nielsen, The three-dimensional structure of CsmA: a small antenna protein from the green sulfur bacterium *Chlorobium tepidum*, FEBS Lett. 582 (2008) 2869–2874.
[23] S.J. Theroux, T.E. Redlinger, R.C. Fuller, S.J. Robinson, Gene encoding the 5.7-kilodalton chlorosome protein of *Chloroflexus aurantiacus*: regulated message levels and a predicted carboxy-terminal protein extension, J. Bacteriol. 172 (1990) 4497–4504.
[24] D.A. Bryant, A.M. Costas, J.A. Maresca, A.G. Chew, C.G. Klatt, M.M. Bateson, L.J. Tallon, J. Hostetler, W.C. Nelson, J.F. Heidelberg, D.M. Ward, *Candidatus Chloracidobacterium thermophilum*: an aerobic phototrophic acidobacterium, Science 317 (2007) 523–526.
[25] M.O. Pedersen, J. Linnanto, N.U. Frigaard, N.C. Nielsen, M. Miller, A model of the protein–pigment baseplate complex in chlorosomes of photosynthetic green bacteria, Photosynth. Res. 104 (2010) 233–243.
[26] J. Pšenčík, A.M. Collins, L. Liljeroos, M. Torkkeli, P. Laurinmäki, H.M. Ansink, T.P. Ikonen, R.E. Serimaa, R.E. Blankenship, R. Tuma, S.J. Butcher, Structure of chlorosomes from the green filamentous bacterium *Chloroflexus aurantiacus*, J. Bacteriol. 191 (2009) 6701–6708.
[27] J. Moll, S. Daehne, J.R. Durrant, D.A. Wiersma, Optical dynamics of excitons in *J* aggregates of a carbocyanine dye, J. Chem. Phys. 102 (1995) 6362–6370.
[28] G.T. Oostergetel, M. Reus, A. Gomez Maqueo Chew, D.A. Bryant, E.J. Boekema, A.R. Holzwarth, Long-range organization of bacteriochlorophyll in chlorosomes of *Chlorobium tepidum* investigated by cryo-electron microscopy, FEBS Lett. 581 (2007) 5435–5439.
[29] J. Pšenčík, T.P. Ikonen, P. Laurinmäki, M.C. Merckel, S.J. Butcher, R.E. Serimaa, R. Tuma, Lamellar organization of pigments in chlorosomes, the light harvesting complexes of green photosynthetic bacteria, Biophys. J. 87 (2004) 1165–1172.
[30] S. Ganapathy, G.T. Oostergetel, P.K. Wawrzyniak, M. Reus, A. Gomez Maqueo Chew, F. Buda, E.J. Boekema, D.A. Bryant, A.R. Holzwarth, H.J.M. de Groot, Alternating syn-anti bacteriochlorophylls form concentric helical nanotubes in chlorosomes, Proc. Natl. Acad. Sci. U. S. A. 106 (2009) 8525–8530.
[31] R.G. Feick, M. Fitzpatrick, R.C. Fuller, Isolation and characterization of cytoplasmic membranes and chlorosomes from the green bacterium *Chloroflexus aurantiacus*, J. Bacteriol. 150 (1982) 905–915.
[32] W. Fritzsche, A. Schaper, T.M. Jovin, Probing chromatin with the scanning force microscope, Chromosoma 103 (1994) 231–236.
[33] G.A. Montano, B.P. Bowen, J.T. Labelle, N.W. Woodbury, V.B. Pizziconi, R.E. Blankenship, Characterization of *Chlorobium tepidum* chlorosomes: a calculation of bacteriochlorophyll *c* per chlorosome and oligomer modeling, Biophys. J. 85 (2003) 2560–2565.
[34] Y.W. Zhu, B.L. Ramakrishna, P.I. Van Noort, R.E. Blankenship, Microscopic and spectroscopic studies of untreated and hexanol-treated chlorosomes from *Chloroflexus aurantiacus*, Biochim. Biophys. Acta Bioenerg. 1232 (1995) 197–207.
[35] F. Tokumasu, A.J. Jin, J.A. Dvorak, Lipid membrane phase behaviour elucidated in real time by controlled environment atomic force microscopy, J. Electron Microsc. 51 (2002) 1–9.
[36] Y. Saga, T. Wazawa, T. Nakada, Y. Ishii, T. Yanagida, H. Tamiaki, Fluorescence emission spectroscopy of single light-harvesting complex from green filamentous photosynthetic bacteria, J. Phys. Chem. B 106 (2002) 1430–1433.
[37] A. Martinez-Planells, J.B. Arellano, C.A. Borrego, C. Lopez-Iglesias, F. Gich, J.S. Garcia-Gil, Determination of the topography and biometry of chlorosomes by atomic force microscopy, Photosynth. Res. 71 (2002) 83–90.
[38] A. Sridharan, J. Muthuswamy, J.T. Labelle, V.B. Pizziconi, Immobilization of functional light antenna structures derived from the filamentous green bacterium *Chloroflexus aurantiacus*, Langmuir 24 (2008) 8078–8089.
[39] T.M. Wahlund, C.R. Woese, R.W. Castenholz, M.T. Madigan, A thermophilic green sulfur bacterium from New Zealand hot springs, *Chlorobium tepidum* sp. nov. Arch. Microbiol. 156 (1991) 81–90.
[40] D. Fotiadis, P. Qian, A. Philippsen, P.A. Bullough, A. Engel, C.N. Hunter, Structural analysis of the RC–LH1 photosynthetic core complex of *Rhodospirillum rubrum* using atomic force microscopy, J. Biol. Chem. 279 (2004) 2063–2068.
[41] S. Scheuring, J. Seguin, S. Marco, D. Levy, C. Breyton, B. Robert, J.L. Rigaud, AFM characterization of tilt and intrinsic flexibility of *Rhodobacter sphaeroides* light harvesting complex 2 (LH2), J. Mol. Biol. 325 (2003) 569–580.
[42] Z. Liu, C.G. Klatt, J.M. Wood, D.B. Rusch, M. Ludwig, N. Wittekindt, L.P. Tomsho, S.C. Schuster, D.M. Ward, D.A. Bryant, Metatranscriptomic analyses of chlorophototrophs of a hot-spring microbial mat, ISME J. 5 (2011) 1279–1290.
[43] H. Li, D.A. Bryant, Envelope proteins of the CsmB/CsmF and CsmC/CsmD motif families influence the size, shape, and composition of chlorosomes in *Chlorobaculum tepidum*, J. Bacteriol. 191 (2009) 7109–7120.
[44] D.A. Bryant, Z. Liu, T. Li, F. Zhao, A. Costas, C. Klatt, D. Ward, N.U. Frigaard, J. Overmann, Comparative and functional genomics of anoxygenic green bacteria from the taxa *Chlorobi*, *Chloroflexi*, and *Acidobacteria*, in: R. Burnap, W. Vermaas (Eds.), Functional Genomics and Evolution of Photosynthetic Systems, Springer, Netherlands, 2012, pp. 47–102.
[45] C.A. Gomez Maqueo, N.U. Frigaard, D.A. Bryant, Bacteriochlorophyllide *c* C-8^2 and C-12^1 methyltransferases are essential for adaptation to low light in *Chlorobaculum tepidum*, J. Bacteriol. 189 (2007) 6176–6184.
[46] P.G. Adams, C.N. Hunter, Adaptation of intracytoplasmic membranes to altered light intensity in *Rhodobacter sphaeroides*, Biochim. Biophys. Acta 1817 (2012) 1616–1627.
[47] F. Oesterhelt, D. Oesterhelt, M. Pfeiffer, A. Engel, H.E. Gaub, D.J. Müller, Unfolding pathways of individual bacteriorhodopsins, Science 288 (2000) 143–146.
[48] Y. Saga, Y. Shibata, S. Itoh, H. Tamiaki, Direct counting of submicrometer-sized photosynthetic apparatus dispersed in medium at cryogenic temperature by confocal laser fluorescence microscopy: estimation of the number of bacteriochlorophyll *c* in single light-harvesting antenna complexes chlorosomes of green photosynthetic bacteria, J. Phys. Chem. B 111 (2007) 12605–12609.
[49] Y. Saga, T. Wazawa, T. Mizoguchi, Y. Ishii, T. Yanagida, H. Tamiaki, Spectral heterogeneity in single light-harvesting chlorosomes from green sulfur photosynthetic bacterium *Chlorobium tepidum*, Photochem. Photobiol. 75 (2002) 433–436.
[50] N.U. Frigaard, H. Li, P. Martinsson, S.K. Das, H.A. Frank, T.J. Aartsma, D.A. Bryant, Isolation and characterization of carotenosomes from a bacteriochlorophyll *c*-less mutant of *Chlorobium tepidum*, Photosynth. Res. 86 (2005) 101–111.